DIGITAL HERITAGE (2025)
S. Campana, D. Ferdani, H. Graf, G. Guidi, Z. Hegarty, S. Pescarin, and F. Remondino (Editors)

Comparing MVS and Gaussian Splatting for the 3D Reconstruction of Reflective and Texture-less Cultural Heritage Artifacts

Paolo Clini[1], Roberto Pierdicca[1], Romina Nespeca[1], Renato Angeloni[1], Laura Coppetta[1]

[1] Dept. of Construction, Civil Engineering and Architecture, Università Politecnica delle Marche, Ancona, Italy

Abstract

This study presents a comparative analysis of Multi-View Stereo (MVS) and 3D Gaussian Splatting (GS) for the three-dimensional reconstruction of cultural heritage artifacts characterized by reflective and texture-less surfaces, conditions that traditionally challenge image-based modeling techniques. Two case studies, a ceramic and a bronze head, were documented through controlled photographic acquisition and processed using both methods. Laser scanning served as a geometric benchmark for quantitative evaluation. Results demonstrate that GS provides more spatially homogeneous reconstructions and enhanced visual coherence, particularly in regions affected by specular highlights and low surface texture. Visual comparisons further highlight the potential of GS to deliver smooth, photorealistic renderings through its volumetric, view-dependent representation.

1. Introduction

The three-dimensional digitization of Cultural Heritage (CH) plays a fundamental role in the preservation, study, and dissemination of tangible cultural assets. Over the past decades, image-based modeling techniques, particularly those based on Structure-from-Motion (SfM) and Multi-View Stereo (MVS), have established themselves as accessible, low-cost, and versatile solutions for 3D reconstruction. These techniques enable the production of metrically accurate digital replica of architectural structures and movable artifacts using standard photographic equipment, offering substantial benefits in terms of portability and affordability [CBC*24]; [MKR*23]

Nevertheless, these traditional methods face well-known challenges when applied to surfaces with complex optical properties, such as reflective or texture-less materials. As emphasized in multiple studies, these conditions compromise feature detection and matching, often resulting in noisy, incomplete, or distorted models [KVA13]; [BGP*23].

To mitigate these issues, researchers have explored a variety of solutions, including the use of cross-polarization, projected patterns, HDR imaging, and hybrid workflows that combine multiple acquisition modalities. However, these improvements introduce additional operational complexity and costs, thereby diminishing the efficiency of SfM-MVS approaches. As a result, its affordability and accessibility becomes less evident, making it less advantageous when measured against laser or structured-light scanners, despite the latter still presenting substantial economic constraints for many heritage institutions [NNMR14]; [CNA*23].

In recent years, breakthroughs in machine learning have introduced new possibilities for 3D digitization through neural rendering methods. Among the most notable are Neural Radiance Fields (NeRF) and 3D Gaussian Splatting (3DGS), which have shown the ability to synthesize photorealistic novel views even in challenging scenarios. NeRF represents a scene as a continuous five-dimensional volumetric function that encodes spatial position and viewing direction to return color and opacity. This framework enables accurate modeling of view-dependent effects such as reflections and lighting variations [MST*21].

While NeRF has demonstrated impressive rendering quality, it still suffers from high training times, sensitivity to image orientation accuracy, and the generation of noisy point clouds, which limit its application in metric documentation [MG23]; [BCG*24]. To address some of these shortcomings, 3D Gaussian Splatting has been introduced as a real-time alternative that models the scene using a sparse set of anisotropic Gaussian primitives. This method enables efficient rendering at high frame rates and offers improved performance in terms of material appearance, depth perception, and brightness handling [KKLD23]; [YHZ24].

Comparative studies in the CH domain have started to assess these methods side by side with traditional SfM-MVS workflows. Results indicate that while SfM-MVS still yields superior geometric accuracy, particularly in planar or richly textured scenes, NeRF and 3DGS excel in completeness, visual realism, and efficiency [CNAC24].

In particular, 3DGS has been shown to better handle reflective surfaces and to maintain lower noise levels than NeRF in point cloud output, though with some trade-offs in metric accuracy [JTL*24]. This makes it a promising candidate for applications where real-time rendering, aesthetic quality, or immersive visualization is prioritized, such as in museums, virtual tours, and public engagement platforms.

2. Aim of the research

In this paper, we propose a comparative evaluation of MVS and 3DGS for the 3D reconstruction of CH artifacts. Using laser scans as a reference for geometric accuracy, we aim to quantify the capabilities of each method when dealing with surface materials and geometries that are typically problematic for traditional photogrammetric pipelines. Our analysis will focus on reconstruction fidelity, completeness, surface detail retention, and visual realism, providing a clearer understanding of how these techniques can complement or substitute one another in the documentation of texture-less and reflective surfaces.

Quantitative comparisons will be carried out based on point cloud reconstruction, mesh deviation analysis, and completeness metrics, while qualitative assessments will examine the preservation of surface details and photorealistic rendering

DOI: 10.2312/dh.20253144

capabilities. By systematically comparing these technologies across controlled case studies, this work seeks to clarify their respective advantages and limitations. Ultimately, the goal is to inform best practices for integrating emerging neural rendering techniques into conservation workflows, supporting both scientific documentation and the development of immersive experiences for public engagement and education.

3. Methodology

The present research focuses on two case studies: a ceramic head and a bronze one. Both exhibits have highly reflective surface properties, which are known to pose significant challenges for photogrammetric reconstruction. In particular, the ceramic artifact is characterized by a uniform chromatic appearance, resulting in a scarcity of discernible features necessary for robust feature detection and matching within SfM-MVS pipelines (**Figure 1**).

Figure 1: *The ceramic head (left) and the bronze head of Mars (right) used as case studies.*

The two case-study objects were documented using a digital camera equipped with a full-frame sensor. The camera was mounted on a fixed support in conjunction with a motorized turntable, enabling systematic and uniform image acquisition around the entire object. For each artifact, a total of 72 images were acquired from three distinct viewpoints: a top-down trajectory for the upper surfaces, a frontal trajectory for the lateral surfaces, and a bottom-up trajectory specifically aimed at capturing undercuts. The images were acquired in RAW format to preserve the full radiometric information and subsequently preprocessed using Adobe Camera Raw to apply standardized corrections for white balance, sharpness, and contrast. Additionally, Adobe Photoshop was employed to generate masks for each image, isolating the object from the background and minimizing the influence of non-relevant regions during photogrammetric processing. The two final datasets were processed using Reality Capture. The image alignment process for the bronze head yielded satisfactory results, primarily due to the presence of sufficient features that facilitated robust keypoint detection and matching within the SfM pipeline.

Conversely, the alignment of the ceramic head failed, attributable to its homogeneous surface coloration and the presence of intense specular reflections, both of which significantly limited the extraction of stable and repeatable image features. To mitigate these issues, a second acquisition campaign was conducted, employing cross-polarization techniques. Linear polarizing filters were applied to both the camera lens and the light sources in order to reduce specular highlights and enhance the visibility of surface characteristics. Despite these measures, image alignment remained partially unsuccessful, with a subset of images failing to be aligned. In response, a reduced dataset comprising 24 images was selected, all captured from a top-down perspective. This configuration excluded the use of binary masks and relied on the inclusion of coded targets positioned on the turntable to provide additional spatial references. The presence of these artificial features significantly improved the robustness of the alignment process, ultimately enabling the successful generation of a consistent and complete sparse reconstruction. The image alignment achieved through the SfM pipeline in Reality Capture served as the starting point for both subsequent MVS and GS reconstruction processes. This ensures that any differences observed in the final outputs cannot be attributed to variations in the photogrammetric image registration process. Rather, these differences stem solely from the intrinsic characteristics of the two methodologies applied. Subsequently, a dense point cloud was generated via MVS within the same software environment, whereas for the GS, the internal and external camera parameters were imported in Postshot to generate the 3D GS reconstruction.

In both cases, layer masks were employed to isolate regions of interest and suppress artifacts caused by background interference. The final outputs of the two workflows were exported as point clouds, allowing for a direct comparison between the results of the two methodologies. To establish an accurate geometric reference, laser scanning was performed using a 3DeVOK MT with blue laser technology, with a point density of 0.1 mm and alignment supported by reference markers. Upon completing processing, each object had three distinct datasets: a reference mesh obtained via structured-light scanning, a photogrammetric point-cloud generated through the MVS process, and a point-cloud created using GS. The point-clouds were quantitatively compared with the reference mesh using CloudCompare software (**Figure 2**).

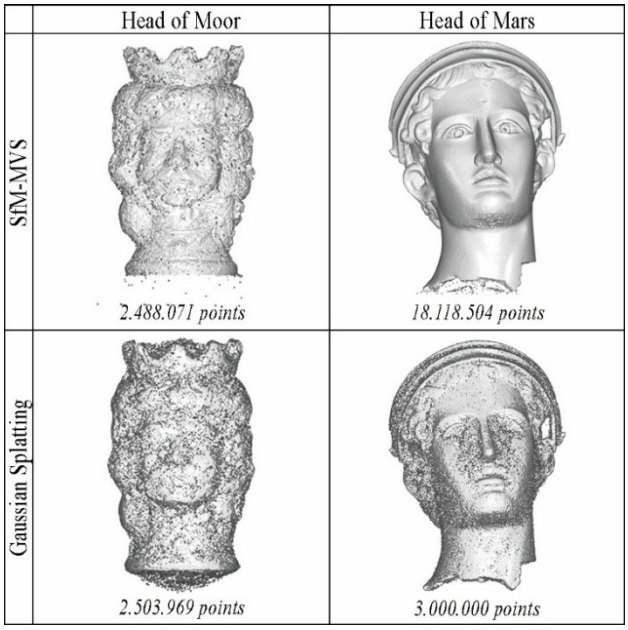

Figure 2: *Point Clouds of the ceramic head (left) and the bronze head of Mars (right).*

This comparative analysis allowed precise evaluation of systematic errors and geometric quality of both techniques, highlighting their strengths and challenges when dealing with texture-less and reflective surfaces. Moreover, to assess the visual quality of the reconstructed models, particularly for applications involving public dissemination, such as museum installations or

online platforms, the MVS workflow was extended to include the generation of textured meshes. The evaluation of visual fidelity focused on comparing these 3D models with the splat-based renderings.

4. Results and discussion

The comparison of the MVS and GS reconstructions against the laser scan reference mesh revealed notable differences in their performance. For the ceramic head, the MVS reconstruction achieved an extremely low mean error with minimal standard deviation, indicating excellent geometric accuracy. Conversely, the GS reconstruction exhibited a slightly higher mean error and a substantially greater standard deviation, suggesting significant difficulties in accurately capturing reflective surfaces.

Similar trends emerged for the bronze head of Mars. The MVS reconstruction once again demonstrated remarkable precision, whereas the GS model showed a higher mean error with a standard deviation comparable to that observed for the ceramic object (**Figure 3**).

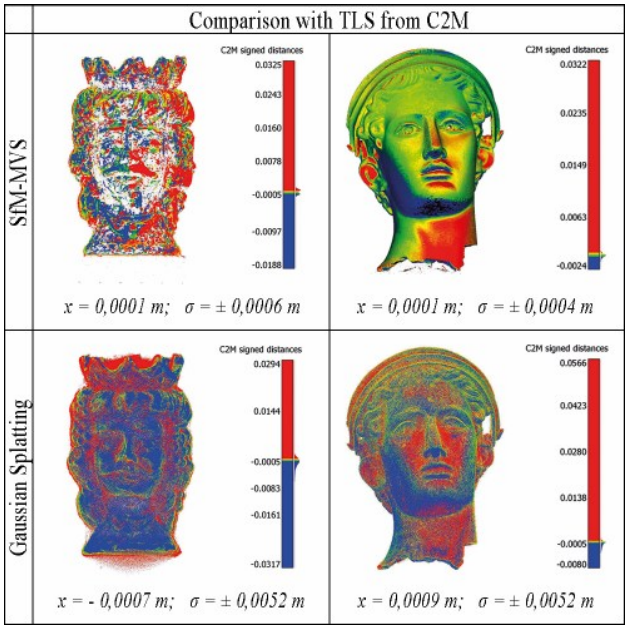

Figure 3: *C2M comparison of the Point Clouds of the heads.*

However, considering the presence of notable outliers in the GS reconstruction characterized by particularly high deviation values, a comparative analysis within a fixed error range of ±0.0005 m revealed that the GS reconstruction remained consistent across the entire object surface. In contrast, the MVS reconstruction exhibited multiple areas lacking sufficient coverage and completeness (**Figure 4**).

Density analysis further emphasized the differences between the two methods. MVS produced dense point clouds characterized by high average densities. In contrast, GS generated reconstructions with notably lower density variability (**Figure 5**). These results further highlight that, despite the presence of surface areas with limited features or the negative impact of specular reflections, GS reconstructions maintain greater spatial uniformity and homogeneity compared to MVS.

The visual comparison between the textured meshes obtained via MVS point cloud and the renderings produced by GS highlighted the effectiveness of Gaussian splats in generating high-quality visualizations. Textured meshes from MVS point cloud exhibited sensitivity to areas lacking sufficient surface features and regions affected by specular reflections, resulting in visible artifacts and noisy geometry. Conversely, GS provided smoother color transitions and more consistent visual rendering of reflective surfaces, benefiting from its volumetric and view-dependent representation.

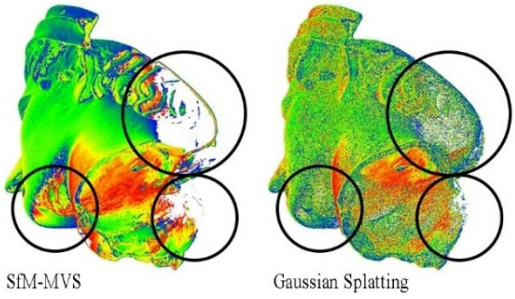

Figure 4: *Point clouds of the bronze head generated using MVS and Gaussian Splatting. Areas not reconstructed by the MVS workflow are clearly highlighted.*

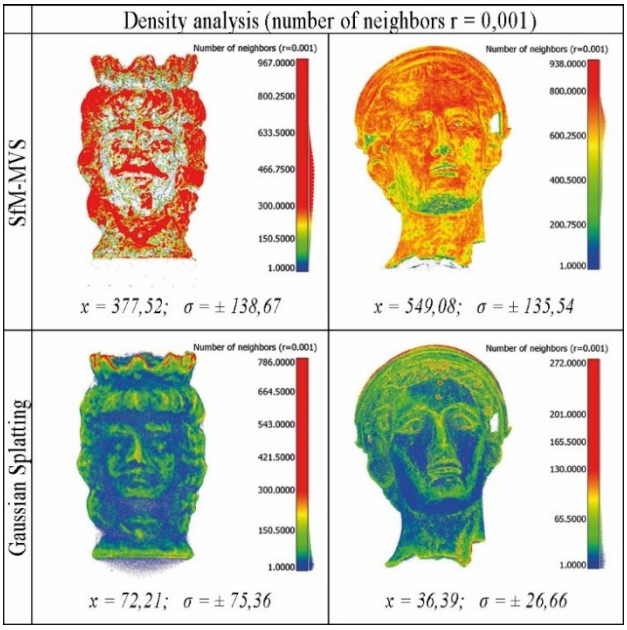

Figure 5: *Density analysis of the Point Clouds of the heads.*

5. Conclusions

The comparative evaluation of MVS and GS in the 3D reconstruction of CH artifacts emphasized the differing capabilities of the two methods when applied to reflective and texture-less surfaces. In both case studies, quantitative analyses against a structured-light laser scan reference demonstrated that, considering the entire reconstructed dataset, MVS outperformed GS in geometric accuracy and point cloud density. Nevertheless, a focused comparative analysis within a restricted deviation threshold (±0.0005 m) revealed that GS yielded more uniform and spatially coherent reconstructions, demonstrating robust performance even under challenging surface conditions, whereas the MVS reconstruction exhibited several unreconstructed areas.

Density analysis further supported these findings, indicating that GS reconstructions exhibited notably lower variability in spatial density distributions, thus enhancing their overall homogeneity. Moreover, qualitative evaluation of the visual

outputs revealed significant differences between the two techniques. MVS textured meshes were susceptible to visual artifacts arising from insufficient surface features and specular reflections, leading to noisy geometry and inconsistencies in surface representation. Conversely, GS provided smoother, more continuous color transitions and visually coherent renderings, benefiting from its volumetric and view-dependent modeling approach. These strengths were particularly pronounced for the ceramic artifact, where GS achieved perceptually consistent visualizations despite a lack of distinctive surface features, and in regions of the bronze head affected by specular reflections.

A rigorous image acquisition workflow combined with a robust SfM process remains essential to ensure geometrically accurate reconstruction of surfaces. However, the subsequent 3D reconstruction using GS has proven to be more effective than traditional MVS techniques, offering a superior response both in terms of geometry and visualization, when considering a narrower and more reliable point interval, which helps mitigate the influence of noise typical of reflective or texture-less surfaces.

Building on the promising results of this study, future research should include a more rigorous quantitative evaluation of radiometric fidelity in GS-based renderings. This may involve the use of perceptual image similarity metrics, color consistency analyses, and reflectance accuracy assessments to better quantify the visual performance of the method. Additionally, given GS's efficiency in real-time rendering, future developments should explore its integration into interactive and immersive platforms such as virtual or augmented reality environments and web-based viewers for museum installations or remote heritage access. Finally, to ensure the long-term usability of GS in cultural heritage workflows, further investigation is needed into the sustainability, interoperability, and archival suitability of splat-based representations, with a focus on data standardization and compatibility with existing digital heritage repositories.

References

[BGP*23] BALLONI, E., GORGOGLIONE, L., PAOLANTI, M., MANCINI, A., & PIERDICCA, R. (2023). Few Shot Photogrametry: a Comparison Between Nerf and Mvs-Sfm for the Documentation of Cultural Heritage. *International Archives of the Photogrammetry, Remote Sensing and Spatial Information Sciences*, *XLVIII-M-2–2023*(M-2–2023), 155–162. https://doi.org/10.5194/ISPRS-ARCHIVES-XLVIII-M-2-2023-155-2023

[BCG*24] BASSO, A., CONDORELLI, F., GIORDANO, A., MORENA, S., & PERTICARINI, M. (2024). Evolution of rendering based on radiance fields.The palermo case study for a comparison between nerf and gaussian splatting. *International Archives of the Photogrammetry, Remote Sensing and Spatial Information Sciences - ISPRS Archives*, *48*(2), 57–64. https://doi.org/10.5194/ISPRS-ARCHIVES-XLVIII-2-W4-2024-57-2024,

[CNAC24] CLINI, P., NESPECA, R., ANGELONI, R., & COPPETTA, L. (2024). 3D representation of Architectural Heritage: a comparative analysis of NeRF, Gaussian Splatting, and SfM-MVS reconstructions using low-cost sensors. *International Archives of the Photogrammetry, Remote Sensing and Spatial Information Sciences - ISPRS Archives*, *48*(2/W8-2024), 93–99. https://doi.org/10.5194/ISPRS-ARCHIVES-XLVIII-2-W8-2024-93-2024,

[CNA*23] CLINI, P., NESPECA, R., ANGELONI, R., D'ALESSIO, M., & MANDOLINI, M. (2023). Combining pattern projection and cross polarization to enhance 3d reconstruction of featureless reflective surfaces. *International Archives of the Photogrammetry, Remote Sensing and Spatial Information Sciences - ISPRS Archives*, *48*(M-2–2023), 427–432. https://doi.org/10.5194/ISPRS-ARCHIVES-XLVIII-M-2-2023-427-2023,

[CBC*24] CROCE, V., BILLI, D., CAROTI, G., PIEMONTE, A., DE LUCA, L., & VÉRON, P. (2024). Comparative Assessment of Neural Radiance Fields and Photogrammetry in Digital Heritage: Impact of Varying Image Conditions on 3D Reconstruction. *Remote Sensing 2024, Vol. 16, Page 301*, *16*(2), 301. https://doi.org/10.3390/RS16020301

[JTL*24] JIANG, Y., TU, J., LIU, Y., GAO, X., LONG, X., WANG, W., & MA, Y. (2024). GaussianShader: 3D Gaussian Splatting with Shading Functions for Reflective Surfaces. *Proceedings of the IEEE/CVF Conference on Computer Vision and Pattern Recognition (CVPR)*, 5322–5332.

[KKLD23] KERBL, B., KOPANAS, G., LEIMKUEHLER, T., & DRETTAKIS, G. (2023). 3D Gaussian Splatting for Real-Time Radiance Field Rendering. *ACM Transactions on Graphics*, *42*(4). https://doi.org/10.1145/3592433

[KVA13] KOUTSOUDIS, A., VIDMAR, B., & ARNAOUTOGLOU, F. (2013). Performance evaluation of a multi-image 3D reconstruction software on a low-feature artefact. *Journal of Archaeological Science*, *40*(12), 4450–4456. https://doi.org/10.1016/J.JAS.2013.07.007

[MKR*23] MAZZACCA, G., KARAMI, A., RIGON, S., FARELLA, E. M., TRYBALA, P., & REMONDINO, F. (2023). Nerf for heritage 3d reconstruction. *International Archives of the Photogrammetry, Remote Sensing and Spatial Information Sciences*, *48*(M-2–2023), 1051–1058. https://doi.org/10.5194/ISPRS-ARCHIVES-XLVIII-M-2-2023-1051-2023

[MST*21] MILDENHALL, B., SRINIVASAN, P. P., TANCIK, M., BARRON, J. T., RAMAMOORTHI, R., & NG, R. (2021). NeRF: Representing Scenes as Neural Radiance Fields for View Synthesis. *Communications of the ACM*, *65*, 99–106. https://doi.org/10.1007/978-3-030-58452-8_24

[MG23] MURTIYOSO, A., & GRUSSENMEYER, P. (2023). Initial assessment on the use of state-of-The-Art nerf neural network 3d reconstruction for heritage documentation. *International Archives of the Photogrammetry, Remote Sensing and Spatial Information Sciences - ISPRS Archives*, *48*(M-2–2023), 1113–1118. https://doi.org/10.5194/ISPRS-ARCHIVES-XLVIII-M-2-2023-1113-2023,

[NNMR14] NICOLAE, C., NOCERINO, E., MENNA, F., & REMONDINO, F. (2014). Photogrammetry applied to problematic artefacts. *International Archives of the Photogrammetry, Remote Sensing and Spatial Information Sciences - ISPRS Archives*, *40*(5), 451–456. https://doi.org/10.5194/ISPRSARCHIVES-XL-5-451-2014,

[YHZ24] YE, K., HOU, Q., & ZHOU, K. (2024). 3D Gaussian Splatting with Deferred Reflection. *Proceedings - SIGGRAPH 2024 Conference Papers*. https://doi.org/10.1145/3641519.3657456/SUPPL_FILE/PAPERS_659_3D